Photoelectrochemistry of Some Aluminum Phthalocyanines in Regenerative Solar Cells

D. Guay* **and J. P. Dodelet****

INRS-Energie, Varennes, Québec, Canada J0L 2P0

R. Côté and C. H. Langford

Chemistry Department, Concordia University, Montréal, Québec, Canada

D. Gravel

Département de chimie, Université de Montréal, Montréal, Québec, Canada

ABSTRACT

Chloroaluminum phthalocyanine (ClAlPc) films sublimed with a high growth rate on SnO_2 can be made to undergo two transformations when the films are in contact with an acidic (HCl) aqueous solution: transformation I is obtained if the solution contains I_3-/I_- and transformation H occurs when there is no redox couple in the solution. The short-circuit photocurrents produced by these two transformations are different. The highest J_{sc} (1.1 mA cm^{-2}), under 100 mW cm^{-2} white light illumination, was measured for transformation I. An investigation of the differences between the initial and the highly photoactive film shows that transformation I induces the growth of an 840 nm band in both absorption and action spectra. Moreover, IR spectroscopy suggests that there is a possible protonation of a peripheral nitrogen of the phthalocyanine macrocycle. This explains the *p*H-dependent kinetics of transformation I, which is larger at lower *p*H. μ-oxo-dimeric aluminum phthalocyanine (PcAlOAlPc) and ClAlPc deposited at a slow growth rate can undergo transformation I but to a lesser extent than high growth rate ClAlPc. Their photoactivities are smaller and their *J*-*V* characteristics indicate an increase of J_0 after transformation of the film, as in the case of the high growth rate ClAlPc. A fluoroaluminum phthalocyanine film does not undergo any transformation I upon contact with an I_3-/I_- acidic aqueous solution. Also, there is no rectification for this film and its photoactivity is very low. Scanning electron micrographs (SEM) reveal morphology differences between films of different phthalocyanines but no differences are observed by SEM, for the phthalocyanine films, before and after transformation I or H.

Among all of the molecular semiconductors tested for energy conversion, only a few have definitely shown to be promising (1). Among those, phthalocyanines (Pcs) have been extensively studied. Under white light illumination, they yield high conversion efficiencies compared to other organic semiconductors. The best results are obtained for dry cells. At 75 mW cm^{-2}, a conversion efficiency of 0.95% has been measured with a two-layer organic photovoltaic cell (CuPc in contact with a perylene tetracarboxylic derivative). Typical cell parameters are J_{sc} = 2.3 mA cm^{-2}, V_{oc} = 450 mV, and *ff* = 0.65 (2).

Wet cells using Pcs have also been analyzed (3-9). They are usually less performing. The best wet junction was obtained by using two chlorogallium phthalocyanines (ClGaPc) electrodes with different doping levels in contact with $Fe(CN)_6^{4-/3-}$ at *p*H 4. It is characterized by a conversion efficiency of 0.11%, under a 75 mW cm^{-2} illumination (8). For comparison, a single electrode of titanyl phthalocyanine (OTiPc) in contact with saturated anthraquinone sulfonate at *p*H 4 yields a power conversion efficiency of 0.08% under an illumination of 250 mW cm^{-2}. Typical cell parameters for this electrode are: J_{sc} = 1.14 mA cm^{-2}, V_{oc} = 0.45V, and *ff* = 0.4 (9).

Recently, we reported results for chloroaluminum phthalocyanine (ClAlPc) films in contact with I_3-/I_- at *p*H 3.2 (10). High short-circuit photocurrents (1.1 mA cm^{-2}) were measured under an illumination of 100 mW cm^{-2}. For the same electrode, V_{oc} = 105 mV and *ff* = 0.35 were obtained. These parameters yield a conversion efficiency of 0.04%. The maximum efficiency is 0.10% at 3 mW cm^{-2}. It is important to note here that these parameters are measured after a slow transformation of the ClAlPc electrode in contact with the acidic solution containing the redox couple. This transformation occurs over a period of several hours, in the darkness or under illumination. It appears to involve permanent changes in the geometric and electronic structure of the Pc films that can be followed spectroscopically or photoelectrochemically.

With the aim of improving the energy conversion efficiency of molecular semiconductors, it is of interest to find out the factors governing the photoelectrochemical improvement of the ClAlPc films during their transformation. As a first approach towards this goal, the effects of the substrate, the sublimation temperature on ClAlPc film formation, the presence or absence of I_3-/I_- in the acidic electrolyte contacting ClAlPc, are analyzed using visible and infrared absorption spectra, action spectra, and scanning electron microscopy. Then, the ClAlPc behavior is compared with that of FAlPc, HOAlPc, and PcAlOAlPc in contact with the same solutions.

Experimental

Materials.—ClAlPc is synthesized by a procedure similar to that described by Owen and Kenney (11) except that the solvent is replaced by a (1/1) mixture of nitrobenzene and quinoline. Both nitrobenzene and quinoline (dried on CaH_2) were distilled under a N_2 atmosphere. The crude ClAlPc is successively washed with toluene, acetone, and methanol before being sublimed under vacuum. Two sublimation rings are observed in the tube. The dye in the colder part of the tube is a dense deposit. It corresponds to ClAlPc. A film of purple needles condenses in the warmer region. It corresponds to PcAlOAlPc. Each compound is collected and sublimed once more before being analyzed. Elemental analysis for the Pcs are reported in Table I along with calculated values.

It is possible to vary the relative proportions of these two compounds by a prolonged extraction of the crude ClAlPc in a soxhlet, using acetronitrile (two days) followed by methanol (one day). This treatment probably increases the hydration of the ClAlPc. Under the influence of temperature during the sublimation step, the hydrated form is then transformed into the dimer (12).

Another synthetic pathway, using Li_2Pc, was also used to prepare ClAlPc. This route was abandoned because the conversion of Li_2Pc to ClAlPc was never complete as demonstrated by the elemental analysis of Al and by the solution absorption spectrum in chloronaphtalene of the re-

---

* Electrochemical Society Student Member.
** Electrochemical Society Active Member.

Downloaded on 2015-03-07 to IP 142.150.190.39 address. Redistribution subject to ECS terms of use (see ecsdl.org/site/terms_use) unless CC License in place (see abstract).

Table I. Measured (M) and calculated (C) elemental analysis, in percent, of the synthesized phthalocyanines

	ClAlPc		PcAlOAlPc		HOAlPc		FAlPc	
	M	C	M	C	M	C	M	C
Al[a]	4.7	4.8	4.8	4.9	4.8	4.8	4.7	4.7
C	66.79	66.84	70.32	70.20	69.00	68.89	68.76	68.80
H	2.72	2.81	3.04	2.95	3.08	3.25	2.69	2.86
N	19.50	19.49	20.50	20.40	20.13	20.00	20.53	20.06
Cl	6.06	6.17	≤0.05	0	—	—	—	—
F	—	—	—	—	—	—	3.41	3.40

[a] The Al content was determined by neutron activation analysis.

sulting Pc. In this case, the Q band shows two large peaks characteristic of the presence of a molecule with D_{2h} symmetry.

Hydroxyaluminum phthalocyanine (HOAlPc) is synthesized from purified ClAlPc. Typically, 5g of ClAlPc are heated to reflux in 50 ml of pyridine and 30 ml of NH_4OH for 24h. After filtration, the product is washed with a 0.1*M* solution of HCl, rinsed with methanol, and dried in an oven.

Fluoroaluminum phthalocyanine (FAlPc) is synthesized from HOAlPc (13). Typically, 30 ml of 48% HF are added to 2g of HOAlPc. This mixture is sonicated overnight. The HF solution is evaporated and the same treatment is repeated a second time. The final product is sublimed under vacuum.

Elemental analyses of HOAlPc and FAlPc are given in Table I.

Electrode preparation.—The Pc films are obtained by sublimation under vacuum (1×10^{-5} torr) in a quartz vessel. The films are deposited onto highly conducting SnO_2 substrates ($\rho_s \simeq 25\text{-}30\ \Omega\ \text{sq}^{-1}$). The distance between the powder and the substrate is 10 cm. With this setup, there is no control of the substrate temperature. The sublimation temperature of the different Pcs is adjusted between 300° and 400°C to provide the same growth rate (~2000 Å min^{-1}) for all dyes. During the course of one sublimation, the experimental setup enables the deposition of six pairs of films with varying thicknesses.

For ClAlPc, a sublimation at reduced sublimation temperature (230°-240°C) on a hot substrate (~200°C) was also performed. In that case, the growth rate was reduced to 300-400 Å h^{-1}. When this slowly grown ClAlPc will be used, it will be explicitly mentioned. All other references to ClAlPc will concern the high growth rate film.

Electrochemical and IR measurements.—Details of the electrochemical measurements have been described elsewhere (6). All short-circuit photocurrents were recorded with an I_3^-/I^- aqueous acidic solution ($[I_3^-] = 0.005M$, $[I^-] = 0.4M$).

All IR spectra were taken with a conventional double beam IR spectrophotometer. Except when KBr pellets were used for the powders, all spectra were recorded as thin films sublimed on a KRS-5 (thallium bromide-iodide) crystal.

Results

Evolution of optical densities and incident quantum yields of ClAlPc.—Optical densities.—Curve A of Fig. 1 presents the absorption spectrum of a 0.16 μm thick ClAlPc film. Two transformations of the initial absorption spectrum can be induced by putting the film in contact with electrolytic solutions. Transformation I (curve B of Fig. 1) or H (curve C of Fig. 1) is observed depending on whether or not the aqueous acidic solution (HCl) contains the I_3^-/I^- redox couple. These transformations are identical to those reported in a previous paper (10). We have changed the way to refer to them (from transformation a to transformation I and transformation b to transformation H) to use a notation that will remind one as to how the film is modified. The initial absorption spectrum of ClAlPc shows a maximum around 740 nm and a shoulder around 650 nm. Like most phthalocyanines in the solid state, the ClAlPc absorption spectrum is broad and quite structureless. After transformation I, the absorption spectrum is even broader. A new band appears at 840 nm along with a reduction of the optical density at 650 and 740 nm. Uptake of iodine in the film causes a change of color, from blue to green due to an optical density increase in the 400 nm region. The spectrum of the I_3^-/I^- solution, recorded in a 1 mm optical path cell is characterized by optical densities of 2.25, 1.20, 1.07, 0.6, and 0.05 at 400, 420, 440, 460, and 500 nm, respectively. After transformation H, the initial absorption spectrum widens on both sides and there is no change in the optical density in the 400 nm region. The color of the film remains blue after transformation H. Both transformations occur in darkness as well as under illumination.

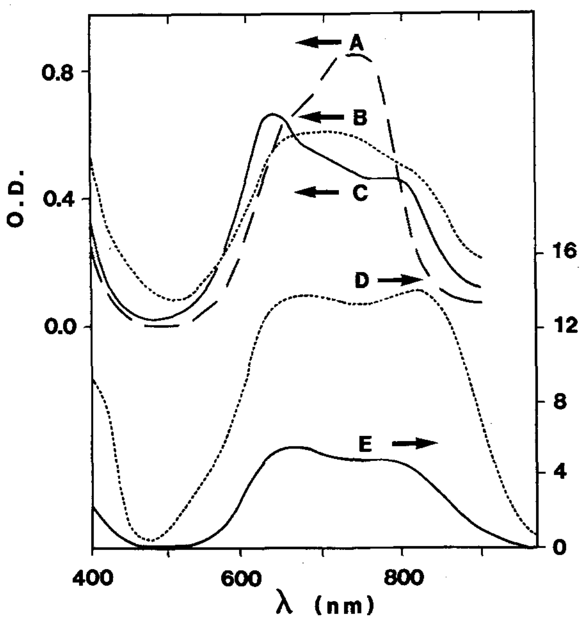

Fig. 1. Absorption spectra (curves A, B, and C) and incident quantum efficiencies φ_i (curves D and E) of a 0.16 μm and ~0.6 μm thick ClAlPc film, respectively; before (A), after transformation I (B, D), and after transformation H (C, E).

The absorption spectrum characteristic of transformation I can be modified further to that of transformation H by putting the film in contact with an aqueous solution at *p*H 3.2. However, the reverse modification is not possible. Once a ClAlPc film has been subjected to transformation H, it is not afterwards able to take up iodine and give the characteristic absorption spectrum of transformation I.

Figure 2 compares the time evolution of the ClAlPc absorption spectrum at two characteristic wavelengths (740 and 840 nm) when a 0.11 μm thick film is undergoing transformation I at two different *p*H values (2.0 and 5.7). The insert in Fig. 2 shows the absorption spectrum of ClAlPc recorded four times after the initial contact of the film with an I_3^-/I^- solution at *p*H 2.0. It takes 4 min to record the complete spectrum and the times indicated on the graph correspond to the beginning of the scan.

Figure 2 illustrates the following points: (*i*) at both *p*H 5.7 and *p*H 2.0, the decrease of optical density (O.D.) at 740 nm (curves A and B) follows the same kinetics as the increase of the 840 nm O.D. (curves D and C). This is confirmed by the presence of an isosbestic point (see insert of Fig. 2); (*ii*) the rate of transformation of the film is influenced by the *p*H value: the lower the *p*H, the greater the transformation rate (curves C and D or curves B and A); (*iii*) a higher O.D. at 840 nm is observed at lower *p*H (curves C and D).

Similar observations have been made for transformation H.

Downloaded on 2015-03-07 to IP 142.150.190.39 address. Redistribution subject to ECS terms of use (see ecsdl.org/site/terms_use) unless CC License in place (see abstract).

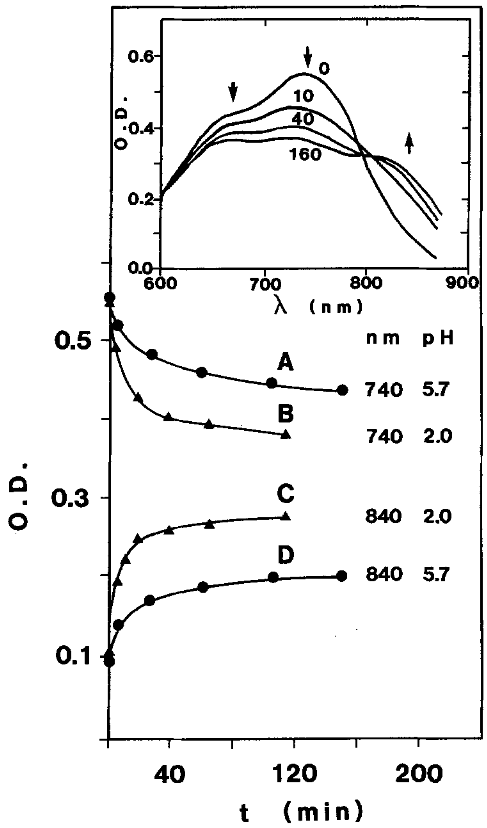

Fig. 2. Time evolution, during transformation I, at pH 2.0 and 5.7, of the optical density at 740 and 840 nm of a 0.11 μm thick ClAlPc film.

Incident quantum yields.—In order to most clearly display the relationship between changing absorption spectra and changing action spectra, the incident quantum yield will be used, defined as

$$\varphi_i(\%) = \frac{\text{number of collected electrons}}{\text{number of incident photons}} \times 100 \qquad [1]$$

In addition, action spectra are normalized for a constant photon flux (3.9×10^{15} photons $cm^{-2}s^{-1}$) using Eq. [2]

$$J_{sc} = kI^{\gamma} \qquad [2]$$

Curves D and E of Fig. 1 show the action spectra of two ~0.6 μm thick ClAlPc films modified following transformations I and H. Those action spectra were recorded at the end of the stabilization period during which the films undergo changes in their absorption spectra. In both cases, an aqueous (pH = 3.2) solution of I_3-/I_- was used to measure the short-circuit photocurrent.

Monochromatic illumination intensities are in the 0.1 mW cm^{-2} range. At these intensities, a value of $\gamma = 0.97$ has been found and used in Eq. [2]. In the case of transformation I (curve D), $\varphi_i \geq 10\%$ for $610 \leq \lambda \leq 880$ nm, which is much larger than the values obtained for transformation H. Both action spectra have the same shape and show a distinct peak above 800 nm at a wavelength corresponding to the shoulder in their respective absorption spectra.

Figure 3 shows the time evolution of φ_i measured at four characteristic wavelengths (λ = 400, 650, 740, and 840 nm) for a ~0.6 μm thick ClAlPc film undergoing transformation I at pH 3.2. Under these conditions, φ_i increases continuously before reaching stabilization. The rate of increase of φ_i is pH dependent, being higher at lower pH. Also, higher quantum yields are obtained at lower pH values. One might wonder why a pH lower than 3.2 was not used on a regular basis on this work. This is because for lower pH, 2.0 for instance, only the thinnest films (≤ 0.1 μm with a maximum O.D. ≤ 0.5) are able to reach stabilization in the way depicted in Fig. 3. At pH 2.0, thicker ClAlPc films show an initial increase of J_{sc} followed by a slow decrease. At the opposite, all the film thicknesses have been found to stabilize with a continuous increase of photocurrent at pH 3.2. Transformation I at this pH therefore allows the optimization of the film photon absorption.

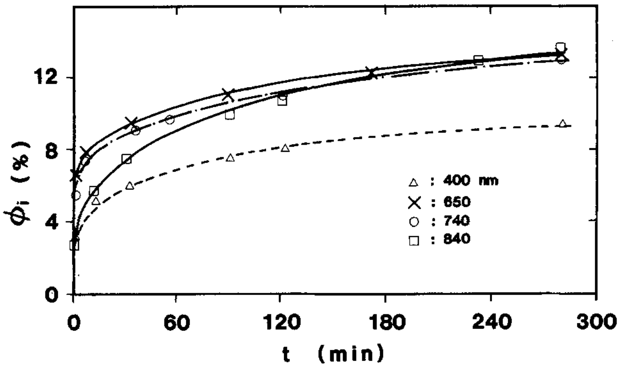

Fig. 3. Time evolution, during transformation I, of φ_i at 400 nm (Δ), 650 nm (X), 740 nm (○), and 840 nm (□), for a 0.6 μm thick ClAlPc film.

It is worth noting here that during film transformation, φ_i increases with time at all wavelengths, even at 650 and 740 nm where the O.D. decreases. A possible explanation could be that there is an overlap between the absorption spectrum of two species, the first one having a major band at 840 nm and minor absorption at lower wavelengths and the other one being responsible for the absorption spectrum of curve A, Fig. 1. This overlap would result in a sharing of the available photons between the two species, the new one being characterized by a higher quantum yield.

Another explanation, which does not necessarily require an overlap between the absorption spectrum of the two species, can be proposed. The 840 nm absorbing species would still be characterized by a high quantum yield; in this scheme, excitation energy at 650 and 740 nm would be transferred to the high quantum yield species, which would then follow its own kinetics of charge transfer. However, if there are two phases present, the situation may be complicated by junction between those phases.

For 0.6 μm thick films of ClAlPc undergoing transformation H, the time evolution behavior of φ_i is different from the one reported in Fig. 3 for a film of same thickness undergoing transformation I. After a transient increase of the photocurrent, there is a stabilization of φ_i near its initial value. The time evolution of φ_i in transformation H cannot be followed continuously. The photocurrent is measured by replacement from time to time of the acidic aqueous solution with an I_3-/I_- solution at pH 3.2 for less than 2 min. The absorption spectrum of the film at the end of the stabilization is characteristic of transformation H despite repeated contacts with I_3-/I_- during the measure of the photocurrents.

Since transformation I yields the highest photocurrent, the effect of film thickness has been studied at pH 3.2. Figure 4 presents these results obtained under white light illumination at 35 mW cm^{-2}. There is a slow variation of J_{sc} for film thicknesses in the range of 0.2-0.8 μm. However, J_{sc} drops very drastically for films thinner than 0.2 μm. Under white light illumination of 100 mW cm^{-2}, the best cells yield a J_{sc} as high as 1.1 mA cm^{-2}.

Quinhydrone ([Benzoquinone] = [Hydroquinone] = $2.5 \times 10^{-3}M$) at pH 3.2 induces spectroscopic modifications of the ClAlPc film similar to the ones reported for transformation I (curve B of Fig. 1) except for the 400-500 nm region which remains unchanged. However, with this redox, J_{sc} values are lower by a factor of 5-6 compared to those obtained with I_3-/I_- even if a small increase in V_{oc} is observed by using quinhydrone (106 mV compared to 80 mV at 35 mW cm^{-2}).

$Fe(CN)_6^{3-/4-}$ (2.5×10^{-3} M/2.5×10^{-3} M) at pH 3.2 induces spectroscopic modifications of the ClAlPc film similar to the ones reported for transformation H (curve C of Fig. 1). J_{sc} and V_{oc} values are very low with this redox mainly due to the film porosity and the reversibility of $Fe(CN)_6^{3-/4-}$ on SnO_2.

Downloaded on 2015-03-07 to IP 142.150.190.39 address. Redistribution subject to ECS terms of use (see ecsdl.org/site/terms_use) unless CC License in place (see abstract).

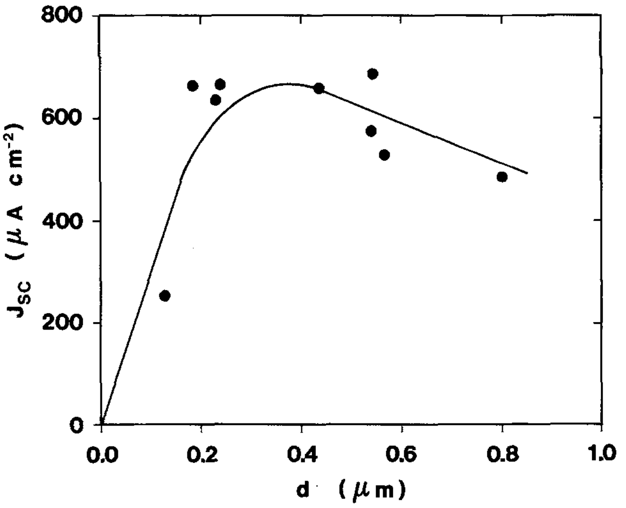

Fig. 4. Variation of J_{sc} (white light illumination at 35 mW cm^{-2}) as a function of the thickness of ClAlPc after completion of transformation I.

In the remaining of this work, I_3^-/I^- will be the only redox used in the photoelectrochemistry measurements.

Optical density and incident quantum yields of slowly grown ClAlPc, and rapidly grown HOAlPc, PcAlOAlPc, and FAlPc.—Curve A of Fig. 5 shows the absorption spectrum of a 0.16 μm thick ClAlPc film deposited on hot substrate (200°C) at a growth rate of 300-400 Å h^{-1}. This absorption spectrum differs in several respects from that of high growth rate ClAlPc presented in Fig. 1 (curve A). It shows a greater absorbancy in the blue (400-500 nm) and near infrared regions (750-900 nm) of the spectrum than does the absorption spectrum of high growth rate ClAlPc. Conditions prevailing during the deposition of ClAlPc greatly influence the absorption spectrum of the film.

Curve B of Fig. 5 presents the absorption spectrum of slowly grown ClAlPc after soaking in a I_3^-/I^- aqueous solution at *p*H 3.2. There are only minor changes between spectra A and B. These changes are similar to those described in Fig. 1 when a ClAlPc film undergoes transformation I, although they are much less important for slowly grown ClAlPc.

Curve C of Fig. 5 shows the action spectrum of slowly grown ClAlPc after transformation of the film with an I_3^-/I^- aqueous solution at *p*H 3.2. Surprisingly, this action spectrum has exactly the same shape as that of high growth rate ClAlPc undergoing transformation I (curve D, Fig. 1). In the present case, the O.D. maximum at 800 nm and the large absorption at 400 nm do not give rise to any corresponding enhancement of the photocurrent. From the comparison between curves B and C of Fig. 5, it could be inferred that the film corresponding to spectrum B is composed of at least two species, one of these (the one responsible for the absorption increase at 400 and 800 nm) being inactive or poorly photoactive. Furthermore, there is a large difference in the time required to achieve completion of transformation I between both ClAlPc films; it takes 45h for slowly grown ClAlPc films compared to 2-4h for the high growth rate ClAlPc films. During that period, the increase of φ_i is roughly the same for both types of ClAlPc films. This difference will be explaned in the microscopy work reported below.

The white light J_{sc} value at 35 mW cm^{-2} for this 0.16 μm thick slowly grown ClAlPc film is 230 μA cm^{-2} compared to J_{sc} = 480 μA cm^{-2} (Fig. 4) for the high growth rate ClAlPc film of same thickness.

PcAlOAlPc.—Curve A of Fig. 6 shows the absorption spectrum of a 0.32 μm thick PcAlOAlPc film. The O.D. maximum occurs at about 625 nm with a shoulder around 725 nm. Soaking the film in I_3^-/I^- does not give rise to any major changes in its absorption spectrum (curve B of Fig. 6). Curve C of Fig. 6 displays the action spectrum of the film in contact with an I_3^-/I^- solution at *p*H 3.2. The action spectrum is in accordance with the absorption spectrum. The white light J_{sc} value at 35 mW cm^{-2} is 245 μA cm^{-2}, compared to J_{sc} = 670 μA cm^{-2} for the high growth rate ClAlPc film of same thickness (Fig. 4).

HOAlPc.—It is not possible to obtain a pure HOAlPc film by sublimation of HOAlPc powder. This was first indicated by the complete coincidence between the absorption and the action spectra of "HOAlPc" and PcAlOAlPc films. The suspicion was confirmed by IR measurements. IR spectra of HOAlPc and PcAlOAlPc powder were measured from 250 to 4000 cm^{-1}. Two major differences can be seen from a comparison of those spectra. HOAlPc powder

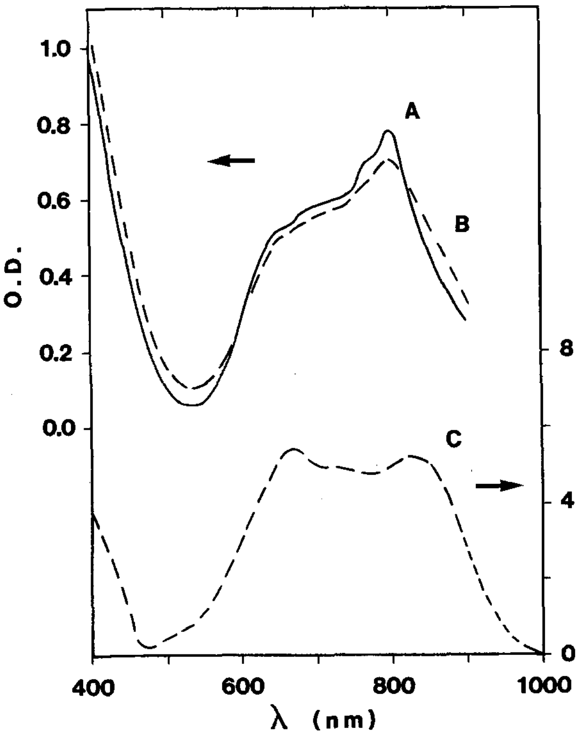

Fig. 5. Absorption spectra (curves A and B) and incident quantum efficiencies, φ_i, (curve C) of a 0.16 μm thick ClAlPc film slowly grown on hot SnO$_2$ before (A) and after transformation I (B and C).

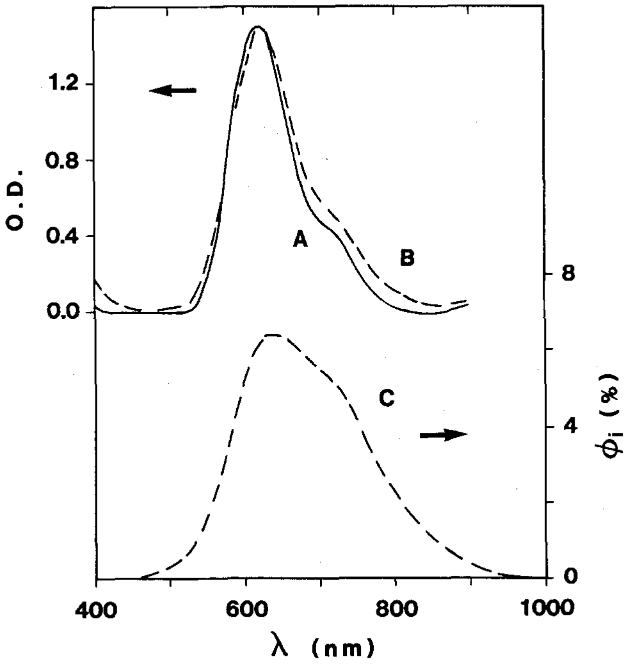

Fig. 6. Absorption spectra (curves A and B) and incident quantum efficiencies, φ_i, (curve C) of a 0.32 μm thick PcAlOAlPc film; before (A) and after transformation I (B and C).

Downloaded on 2015-03-07 to IP 142.150.190.39 address. Redistribution subject to ECS terms of use (see ecsdl.org/site/terms_use) unless CC License in place (see abstract).

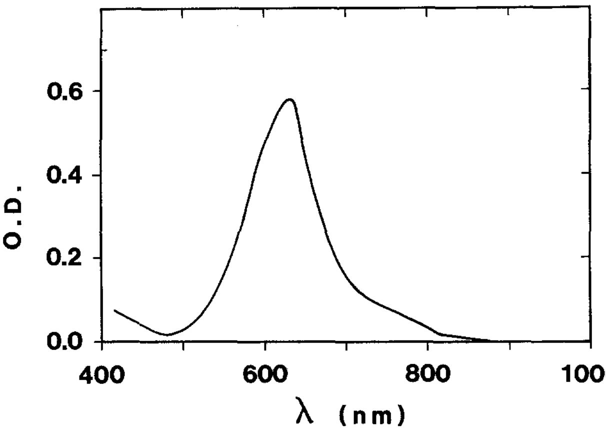

Fig. 7. Absorption spectrum of a 0.12 μm thick FAlPc film before and after transformation I.

shows a broad band related to the OH vibration extending from 3100 to 3650 cm^{-1} with a maximum at 3420 cm^{-1}. This band is much less important in PcAlOAlPc powder. Also, the dimeric Pc shows a band at 1040 cm^{-1} which is lacking in the HOAlPc spectrum. Upon sublimation of both Pc powders as thin films on KRS-5 crystal, both IR spectra show the 1040 cm^{-1} absorption band and no significant absorption in the OH vibration region, indicating that they are mainly composed of the dimer despite the different sources from which they are obtained. This fact would cast some doubt concerning recently published results on the photoelectrochemical behavior of HOAlPc films obtained by sublimation of HOAlPc powder at 530°C (14).

FAlPc.—Figure 7 shows the absorption spectrum of FAlPc. There is no change in the spectrum after contacting the film with I_3-/I_- at *p*H 3.2. Under white light illumination at 35 mW cm^{-2}, the FAlPc film displays a short-circuit photocurrent of only 1.5 μA cm^{-2} compared to 430 μA cm^{-2} for ClAlPc film of the same thickness (Fig. 4). Under these conditions, it was not possible to measure the action spectrum of this compound.

J-V characteristics.—Figure 8 shows the dark *J-V* characteristics of different aluminum phthalocyanine on SnO_2 substrates in contact with an I_3-/I_- solution at *p*H 3.2. The two upper curves are related to ClAlPc and they were measured immediately after the initial contact with the solution (○) and after completion of transformation I (■). With the exception of FAlPc for which the *J-V* curve is given in Fig. 8 (●), all compounds studied (slowly grown ClAlPc and PcAlOAlPc) display the same rectification as ClAlPc. This confirms the semiconducting character (p-type) of such Pc films. Transformation I does not induce major changes in the rectification properties of the film.

For potentials in the forward bias region (E_{redox} = 274 mV), the dark *J-V* curve is described by the following expression

$$J = J_0 \left[\exp \frac{e(V - JR_s)}{kT} - 1 \right] \qquad [3]$$

where J_0 is the exchange current density and R_s the series resistance. Before transformation, a reasonable fit of the *J-V* curve can be obtained by using the following parameters: J_0 = 3 μA cm^{-2} and R_s = 70 Ω cm^2. After completion of transformation I, the dark *J-V* curve is adequately described with J_0 = 13 μA cm^{-2} and R_s = 67 Ω cm^2.

Iodine in the vapor phase (15) or dissolved in hydrocarbon (16) and in water (I_3-) (17) is known to increase the conductivity of various phthalocyanines. However, in the present work, R_s does not decrease after transformation I. If the film area remains constant in transformation I and R_s is not modified, the change in the J_0 value signifies a change of mechanism. In the following section, SEM pictures tend to demonstrate that there is no significant change of the actual film area after transformation of the film with I_3-/I_-.

In the case of FAlPc, the *J-V* curve shows no rectifying behavior, in agreement with the low photocurrent observed for that phthalocyanine. However, the presence of the Pc film on SnO_2 substrate greatly enhances the charge transfer between the electrode and the I_3-/I_- redox under both cathodic and anodic polarizations. For comparison, the *J-V* curve obtained on bare SnO_2 with the same solution is given in Fig. 8 (□). This "catalysis" in comparison to SnO_2 is similar to that described by Crouch and Langford (18) who reported porphyrin films electron exchange rate constants to reach values similar to those of Pt electrodes.

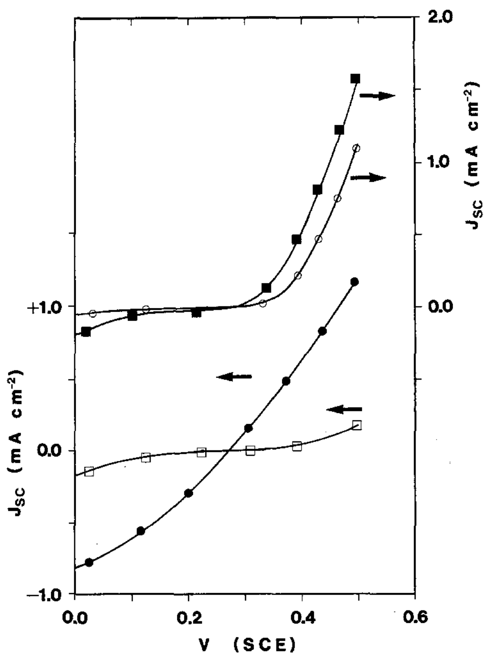

Fig. 8. Dark *J-V* characteristics of a ClAlPc film before (○) and after transformation I (■); of a FAlPc film (●); of bare SnO_2 substrate (□). The redox is I_3-/I_- at *p*H 3.2.

Film morphologies.—Figure 9 presents the SEM of the SnO_2 substrate (9A), along with a 0.10 (9B), 0.24 (9C), and 0.6 μm (9D) thick ClAlPc film on that substrate, at the same magnification. It shows that the morphology of the SnO_2 substrate is respected for the thin (0.10 μm) ClAlPc film. Thicker layers (9C and 9D) develop their own morphology, consisting of dense bundles of small crystallites of about 50 nm in diam. These crystallites are already present in the thinner film (9B). It was shown previously (19) that for films thicker than 9D, the growth involves an increase in the length of the crystallites, while their diameter remains quite constant.

Figure 10 shows the SEM of two ClAlPc films, after transformation I (Fig. 10A) and transformation H (Fig. 10B), at the same magnification. These films have nearly the same thickness: 0.26 μm for 10A and 0.30 μm for 10B. By comparing Fig. 9C, 9D, 10A, and 10B, it can be concluded that the morphology of the ClAlPc film is not affected by transformation I or transformation H.

Figure 11 shows the SEM of slowly grown ClAlPc sublimed onto a hot substrate. This film has a thickness of 0.15 μm, which is between the thicknesses of the high growth rate ClAlPc films depicted in Fig. 9B and 9C. A comparison of those pictures shows that the low growth rate film morphology seems to be quite different from that of the high growth rate film. In this case, the dye crystallites have the same dimension as the SnO_2 substrate crystallites. Similar influence of the growth rate on the film morphology was already reported for ClGaPc (20).

Figure 12A presents the SEM of a 0.12 μm thick FAlPc film. The morphology of this film is similar to that of the one presented in Fig. 11. However, the short-circuit photocurrents differ greatly for those two films: under white light illumination (35 mW cm^{-2}), J_{sc} = 1.5 μA cm^{-2} for FAlPc and J_{sc} = 230 μA cm^{-2} for slowly grown ClAlPc. This demonstrates that the dominant factor behind the photocurrent generation is not the film morphology. This fact is confirmed by comparing Fig. 9C and 9D to Fig. 12B

Downloaded on 2015-03-07 to IP 142.150.190.39 address. Redistribution subject to ECS terms of use (see ecsdl.org/site/terms_use) unless CC License in place (see abstract).

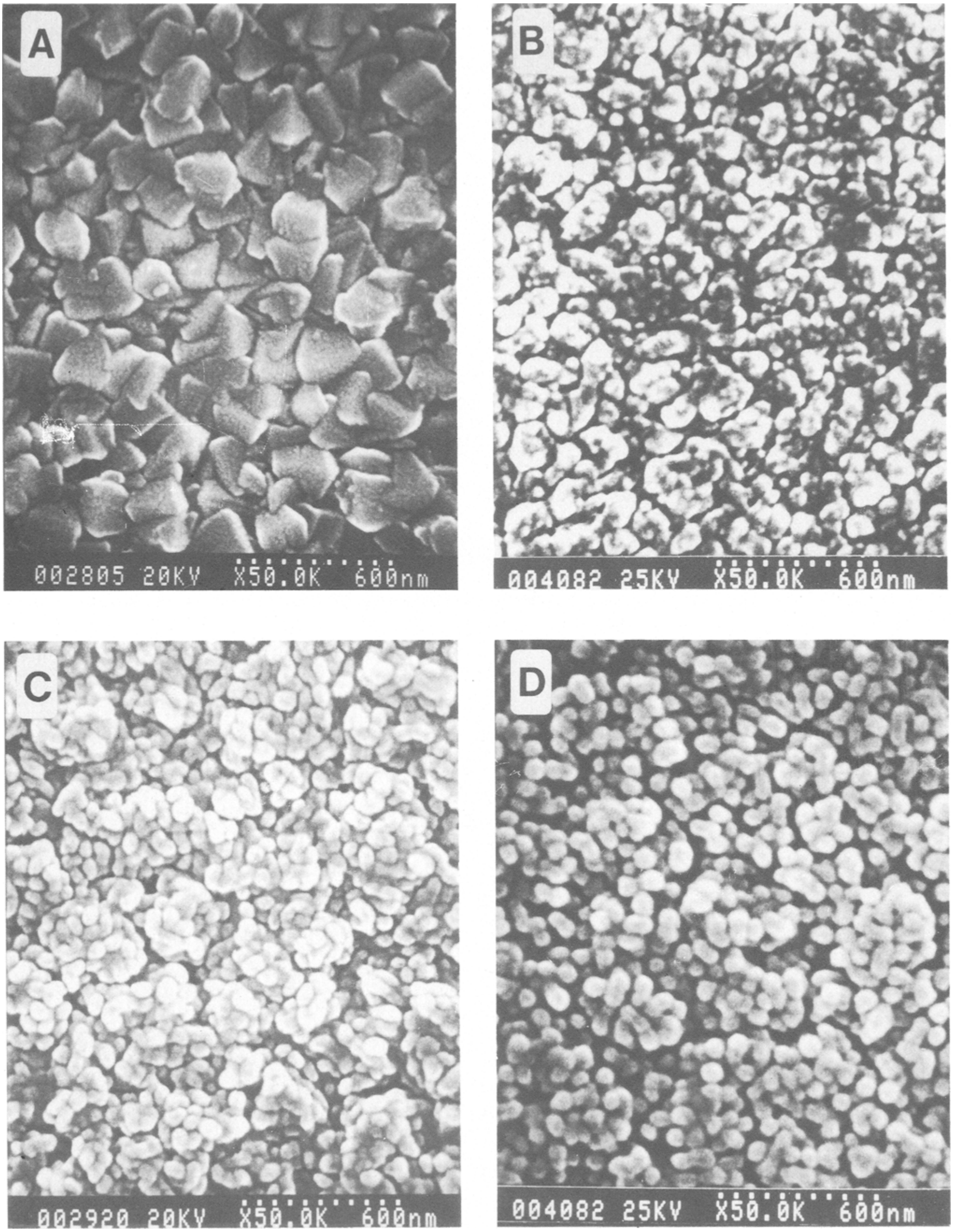

Fig. 9. Scanning electron micrograph of the SnO_2 substrate (A), of a 0.10 (B), 0.24 (C), and 0.60 μm thick ClAlPc film, (D)

which shows the SEM of a 0.32 μm thick PcAlOAlPc film on SnO_2 substrate. Although the actual area of PcAlOAlPc seems to be larger than the one for the high growth rate ClAlPc film, the photocurrent generation is not enhanced: under white light illumination (35 mW cm^{-2}), J_{sc} = 245 μA cm^{-2} for PcAlOAlPc compared to J_{sc} = 670 μA cm^{-2} for the same thickness of ClAlPc.

Infrared measurements.—IR spectra have been recorded for all the Pcs studied in this work by sublimation of a thin film on KRS-5 crystal. Spectra were taken from 250 to 4000 cm^{-1}. Between 1650 and 4000 cm^{-1}, there is a large absorption region due to the presence of water absorbed from the aqueous solutions used for the film transformations. For ClAlPc films, both transformations influence the same ab-

Downloaded on 2015-03-07 to IP 142.150.190.39 address. Redistribution subject to ECS terms of use (see ecsdl.org/site/terms_use) unless CC License in place (see abstract).

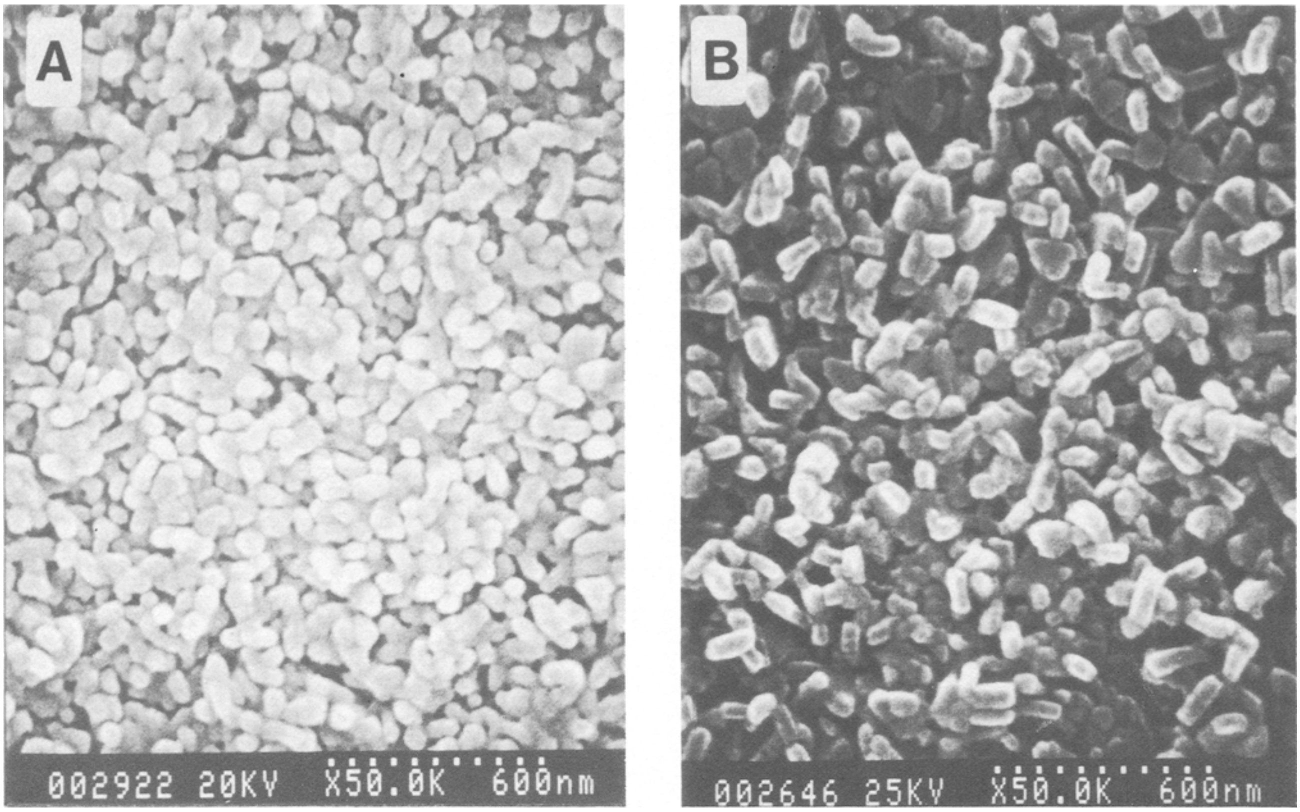

Fig. 10. Scanning electron micrograph of a 0.26 μm thick ClAlPc film after transformation I (A) and a 0.30 μm thick ClAlPc film, after transformation H (B).

sorption bands. However, the changes are more obvious with transformation H and will now be described. After transformation H, new bands appear at 1131 and 1460 cm^{-1}. Bands at 427, 448, and 1060 cm^{-1} disappear. Modifications also occur in the intensity of most other bands, especially in the region between 700 and 800 cm^{-1} which is a sensitive indicator of the crystallographic phase of phthalocyanines (21).

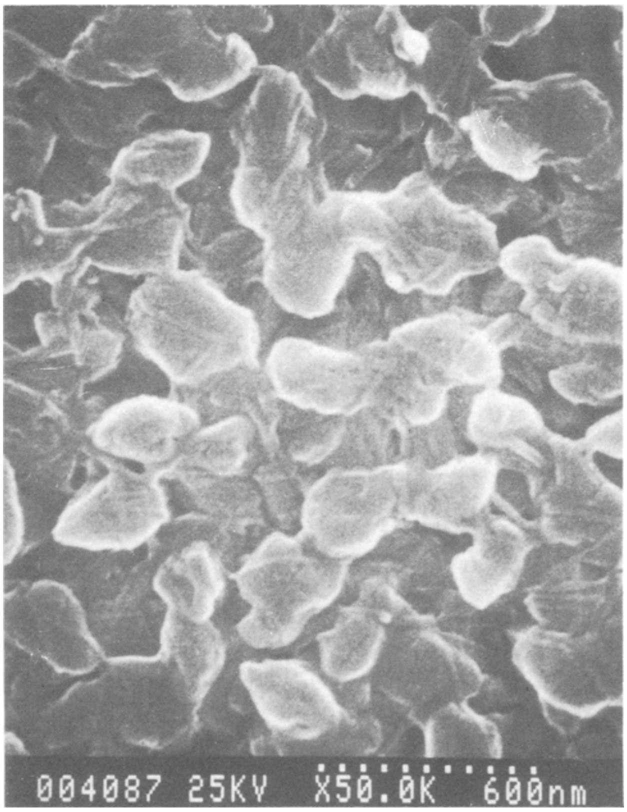

Fig. 11. Scanning electron micrograph of a 0.15 μm thick ClAlPc film slowly grown on a hot substrate.

As far as transformations I and H are concerned, the best documented infrared region is around 900 cm^{-1}, which is shown in Fig. 13A for the initial ClAlPc film. The position of that band remains unchanged for all the Pcs studied in this work (films of FAlPc, ClAlPc, PcAlOAlPc, and also HOAlPc in a KBr pellet). On the other hand, the position of that band shifts when Al is replaced by another metal, moving from 890 cm^{-1} for Mg to 915 cm^{-1} for Co; for H_2Pc, this band is at 874 cm^{-1} (21).

Figures 13B and C show the evolution of the 900 cm^{-1} band after transformations I and H at *p*H 1.0 during 30 min. This *p*H value has been used in order to minimize the contact time between the crystal and the aqueous solution. Indeed, extended contact of the crystal with water results in a loss of IR transmission. The band splitting observed in Fig. 13C is not the result of hydrolysis of the AlCl band since upon ligand exchange, the position of the band remains unmodified. Also, it is not due to demetallation of the Pc since H_2Pc absorbs at 874 cm^{-1}. It therefore appears logical to conclude at this stage that the band splitting at 900 cm^{-1} results from the possible protonation of a peripheral nitrogen atom of the Pc, as described by Sidorov *et al.* (22) for the interaction of a MgPc with acetic acid and HCl. The difference between Fig. 13B and C might originate from the nature of the counterion included in the film if there is protonation. That counterion could be I^-, I_3^-, or Cl^- for transformation I but necessarily Cl^- for transformation H.

Discussion

It has been shown that high growth rate ClAlPc films sublimed on SnO_2 substrate are able to undergo a transformation when put in contact with an I_3^-/I^- acidic solution. This transformation (I) gives rise to an important increase in the energy conversion properties of the pigment. Another ClAlPc transformation (H) has also been identified. It occurs in acidic aqueous media with I_3^-/I^-. The energy conversion properties of the pigment undergoing that latter transformation are not very different from those of the

Downloaded on 2015-03-07 to IP 142.150.190.39 address. Redistribution subject to ECS terms of use (see ecsdl.org/site/terms_use) unless CC License in place (see abstract).

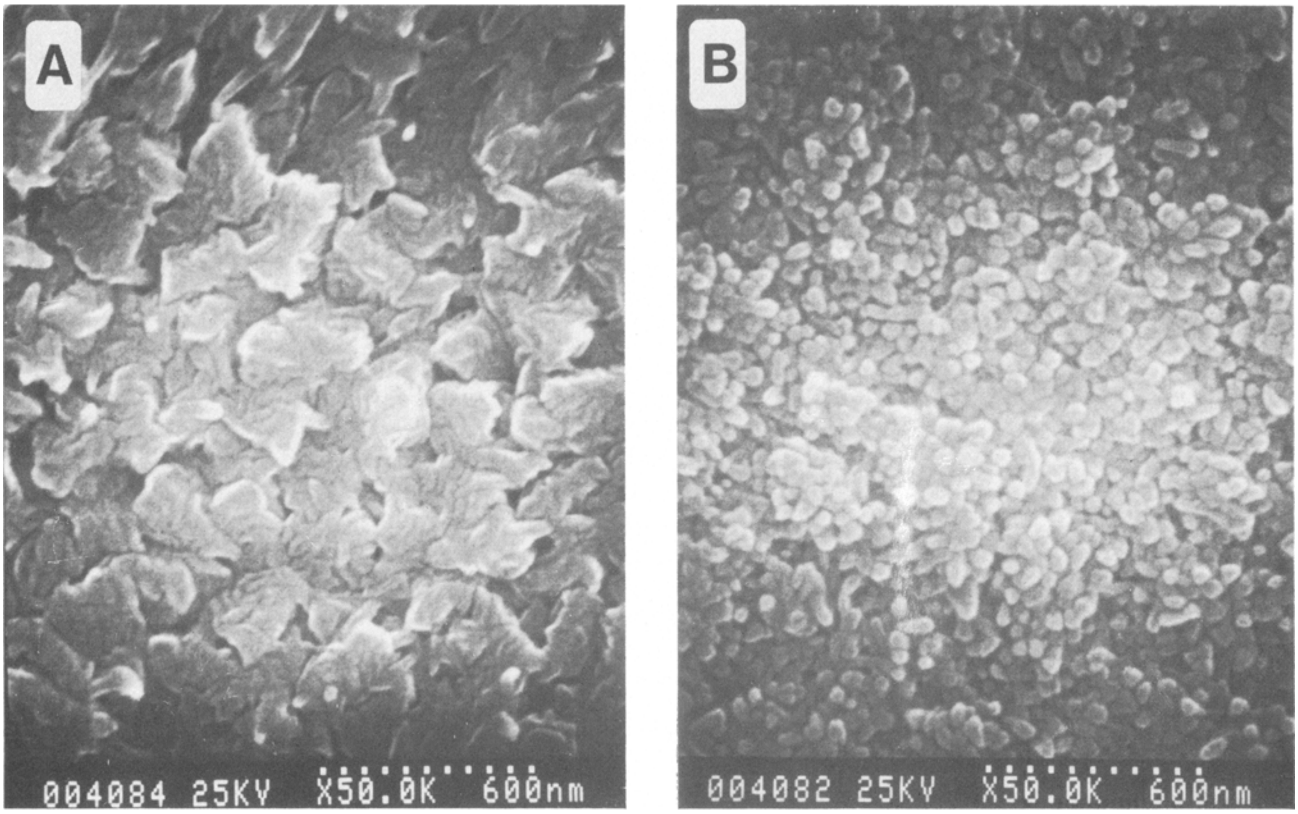

Fig. 12. Scanning electron micrograph of a 0.12 μm thick FAlPc film (A) and a 0.32 μm thick PcAlOAlPc film (B)

initial film. The goal for this work was twofold. First, it was to see if film transformation was a general phenomenon for several aluminum phthalocyanines. The other aim of this work was to find out the differences between initial and transformed films using visible, IR, and action spectroscopies, SEM and electrochemical J-V characterization.

Among the aluminum phthalocyanines studied in this work, it is the high growth rate ClAlPc which shows the most important modifications of its visible spectrum when in contact with I_{3-}/I_{-}. With this modification is the appearance of an 840 nm band in the visible absorption spectrum as well as in the action spectrum.

It has been found that the Q-band region in the absorption spectra of trivalent phthalocyanines is very sensitive to the environment of the molecules. A red-shift of the Q band in the solid state compared to solution absorption has been correlated to enhance photoactivity both in the wet (23) and dry (24) cell configurations. However, the 800 nm absorption maximum appearing in the absorption spectrum of a slowly grown ClAlPc film sublimed onto a hot substrate is absent in the action spectrum which is identical to the one measured for the high growth rate ClAlPc film (with lower φ_i values). Therefore, the presence of a species with an absorption shifted to the near infrared is not sufficient to increase the quantum yield.

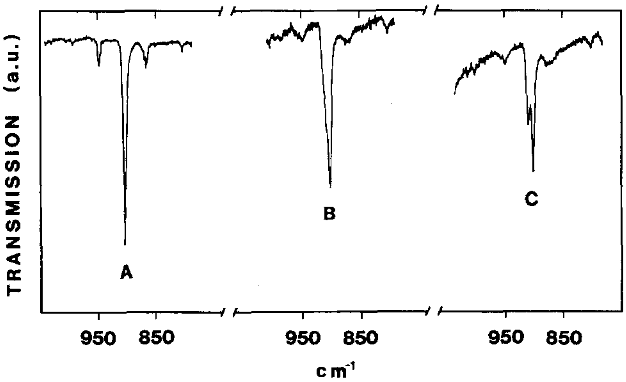

Fig. 13. Evolution of the 900 cm^{-1} infrared band before transformation (A), after transformation I (B), and after transformation II (C) of a ClAlPc film.

Based on IR spectroscopy, it was concluded that both transformations involved possible protonation of the peripheral nitrogens of the Pc macrocycles. This explains the critical effect of pH on the transformation kinetics. Due to the large modification observed in the visible absorption spectrum, protonation does not occur only at the surface of the ClAlPc crystallites revealed by SEM (Fig. 9C and D) but also has to take place in a fraction of the bulk. As proton migration in a solid phase is expected to be quite fast, the slow kinetics (2-4h) of the transformation should reflect some structural reorganization. Comparable changes in the spectroscopy of Pc thin films have been observed by thermal treatment, exposure to organic solvents, acid pasting, and ball milling. They have been described for instance for metal free Pc (25), ZuPc (26), CuPc (27), VOPc (28), MgPc (29), ClGaPc and ClInPc (30). Therefore, one might conclude that structural changes mainly affecting high growth rate ClAlPc may result from the incorporation of protons accompanied by counterion intercalation. This observation also may point out the importance of incorporated impurities in controlling the photoactivity of such thin film electrode materials.

FAlPc is clearly different from all the other phthalocyanines studied in this work and is characterized by a low photoactivity (31). It is the only phthalocyanine measured in this work that does not show any rectification in contact with I_{3-}/I_{-}. The structural reorganization which is reflected by the evolution of the ClAlPc absorption in the visible can also explain why FAlPc does not undergo transformation in the same conditions. Indeed, FAlPc crystallizes as a polymer in a stacked ring structure with an (Al-F)$_x$ backbone (13). The electronegativity of fluorine prevents any modification of that structure. For ClAlPc, it is expected that the strength of the Al-Cl bond is weaker than that of Al-F. This reason and the fact that the halogen is larger in size will cause the ClAlPc to crystallize in a slipped disk structure (32), allowing for structure reorganization upon contact with an acidic electrolytic solution. These structural modifications of ClAlPc do not affect the morphology of the crystallites, at least not at the magnification presented in this work (Fig. 10). However, the different ab-

Downloaded on 2015-03-07 to IP 142.150.190.39 address. Redistribution subject to ECS terms of use (see ecsdl.org/site/terms_use) unless CC License in place (see abstract).

sorption spectra measured for ClAlPc in this study tend to demonstrate that more than one structure can be stabilized for this compound.

Conclusion

The largest increase in energy conversion efficiency occurs for high growth rate ClAlPc films sublimed onto SnO_2 after contact with an I_3-/I_- aqueous acidic solution. This increase involves the appearance of an 840 nm band in both absorption and action spectra and a possible protonation of the peripheral nitrogens of the Pc macrocycle. Experiments are underway to assess if there is a modification of the crystalline structure after transformation of the Pc films and to determine the nature of the counterion necessary to maintain the electric neutrality of the organic semiconductor.

Manuscript submitted April 15, 1988; revised manuscript received Nov. 15, 1988. This was in part Paper 846 presented at the Honolulu, HI Meeting of the Society, Oct. 18-23, 1987.

INRS Energie assisted in meeting the publication costs of this article.

REFERENCES

1. J. Simon and J. J. André, "Molecular Semiconductors," Springer-Verlag, Berlin (1985).
2. C. W. Tang, *Appl. Phys. Lett.*, **48,** 183 (1986).
3. P. Leempoel, F. R. F. Fan, and A. J. Bard, *J. Phys. Chem.*, **87,** 2948 (1983).
4. R. O. Loutfy and L. F. McIntyre, *Sol. Energy Mater.*, **6,** 467 (1982).
5. R. O. Loutfy and L. F. McIntyre, *Can. J. Chem.*, **61,** 72 (1983).
6. D. Bélanger, J. P. Dodelet, L. H. Dao, and B. A. Lombos, *J. Phys. Chem.*, **88,** 4288 (1984).
7. W. J. Buttner, P. C. Rieke, and N. R. Armstrong, *J. Am. Chem. Soc.*, **107,** 3788 (1985).
8. T. Klofta, W. F. Buttner, and N. R. Armstrong, *This Journal*, **133,** 1531 (1986).
9. T. Klofta, J. Danziger, P. Lee, J. Pankow, K. W. Nebesny, and N. R. Armstrong, *J. Phys. Chem.*, **91,** 5646 (1987).
10. D. Guay, R. Côté, R. Marquès, J. P. Dodelet, M. F. Lawrence, D. Gravel, and C. H. Langford, *This Journal*, **134,** 2942 (1987).
11. J. E. Owens and M. E. Kenney, *Inorg. Chem.*, **1,** 331 (1962).
12. J. E. Owens and M. E. Kenney, *ibid.*, **1,** 334 (1962).
13. J. P. Linsky, T. R. Paul, R. S. Nohr, and M. E. Kenney, *ibid.*, **19,** 3131 (1980).
14. G. Perrier and L. H. Dao, *This Journal*, **134,** 1148 (1987).
15. G. A. Chamberlain and P. J. Cooney, *Chem. Phys. Lett.*, **66,** 88 (1979).
16. R. S. Nohr, P. M. Kuznesof, K. J. Wynne, M. E. Kenney, and P. G. Siebenman, *J. Am. Chem. Soc.*, **103,** 4371 (1981).
17. P. Leempoel, M. Castro-Acuna, F. R. F. Fan, and A. J. Bard, *J. Phys. Chem.*, **86,** 1396 (1982).
18. A. M. Crouch and C. H. Langford, *J. Electroanal. Chem.*, **221,** 83 (1987).
19. D. Guay, R. Côté, R. Marques, J. P. Dodelet, M. F. Lawrence, D. Gravel, and C. H. Langford, in "Photoelectrochemistry and Electrosynthesis on Semiconducting Materials," (PV 88-14), D. S. Ginley, K. Honda, A. Nozik, A. Fugishima, N. Armstrong, T. Sakata, and T. Kawai, Editors, p. 287, The Electrochemical Softbound Proceedings Series, Pennington, NJ (1988).
20. P. C. Rieke, C. L. Linkous, and N. R. Armstrong, *J. Phys. Chem.*, **88,** 1351 (1984).
21. A. N. Sidorov and I. P. Kotlyar, *Optics Spectros.* **11,** 92 (1961).
22. A. N. Sidorov and A. N. Terenin, *ibid.*, **11,** 175 (1961).
23. T. J. Klofta, P. C. Rieke, C. A. Linkous, W. J. Buttner, A. Nanthakumar, T. D. Mewborn, and N. R. Armstrong, *This Journal*, **132,** 2134 (1985).
24. A.-M. Hor, R. O. Loutfy, and C. K. Hsiao, *Appl. Phys. Lett.*, **42,** 165 (1983).
25. J. H. Sharp and M. Lardon, *J. Phys. Chem.*, **72,** 3230 (1968).
26. F. Iwatsu, T. Kabayashi, and N. Uyeda, *ibid.*, **84,** 3223 (1980).
27. J. H. Sharp and M. Abkowitz, *ibid.*, **77,** 477 (1973).
28. C. H. Griffiths, M. S. Walker, and P. Goldstein, *Mol. Cryst. Liq. Cryst.*, **33,** 149 (1976).
29. A. M. Hor and R. O. Loutfy, *Thin Solid Films*, **106,** 291 (1983).
30. R. O. Loutfy, A. M. Hor, G. Dipaola-Barangi, and C. K. Hsiao, *J. Imaging Sci.*, **29,** 116 (1985).
31. T. M. Mezza, C. L. Linkous, V. R. Shepard, N. R. Armstrong, R. Nohr, and M. Kenney, *J. Electroanal. Chem.*, **124,** 311 (1981).
32. K. J. Wynne, *Inorg. Chem.*, **23,** 4658 (1984).

Silicon Electrodes Coated with Extremely Small Platinum Islands for Efficient Solar Energy Conversion

Keiichi Ueda, Yoshihiro Nakato, Noriyuki Suzuki, and Hiroshi Tsubomura

Laboratory for Chemical Conversion of Solar Energy and Department of Chemistry, Faculty of Engineering Science, Osaka University, Toyonaka, Osaka 560, Japan

ABSTRACT

Platinum islands 5-50 nm in size were deposited on n-type single-crystal silicon (n-Si) wafers by reduction of hexachloroplatinic (IV) acid (H_2PtCl_6) with hydrogen. Photoelectrochemical solar cells, made from such an n-Si electrode coated with Pt islands, generated open-circuit photovoltages (V_{oc}) as high as 0.63V, about 8% higher than those of normal p-n junction Si solid solar cells. The ideality factor (n) was estimated to be close to unity, and the dark saturation current density (j_s) was estimated to be very low, 2.9×10^{-12} A/cm^2 or less, in accord with the above-mentioned high V_{oc}. Though the V_{oc} obtained here is somewhat lower than the top data reported previously, the relation between the size of the metal island and V_{oc} has been further clarified. These results give further support to our recently proposed theory that the effective barrier height in a Pt-island coated n-Si electrode depends on the island size and can reach the equivalent of the bandgap for small islands. Also, a p-type Si electrode coated with Pt islands in the same way as for the n-Si electrode showed a good rectifying character and an efficient hydrogen evolving photocurrent in an acid solution.

Semiconductor photoelectrochemical (PEC) cells have been attracting attention from the aspect of possible solar energy conversion (1-4). This method has an advantage in that low-cost semiconductor materials such as polycrystalline or amorphous films can be used without loss of efficiency. This method has another advantage in that solar energy can be converted directly into storable chemical energy (fuels).

The main difficulty in this method lies in that almost all known semiconductors having bandgaps matched for the solar energy conversion are photocorroded in aqueous solutions. We have made extensive studies of the stabiliza-

Downloaded on 2015-03-07 to IP 142.150.190.39 address. Redistribution subject to ECS terms of use (see ecsdl.org/site/terms_use) unless CC License in place (see abstract).